# Bone Density and Microstructure of Osseointegration Dental Implants Treated with Uncaria Gambir Roxb Extract Using Periapical Radiography

Mochamad Yoga Dharmawan[1], Farina Pramanik[2]*, Azhari Azhari[2]

1. Dental Undergraduate Study Program, Faculty of Dentistry, Universitas Padjadjaran, Bandung, Indonesia.
2. Department of Dentomaxillofacial Radiology, Faculty of Dentistry, Universitas Padjadjaran, Bandung, Indonesia.

**Abstract**

Radiography is essential in assessing osseointegration, specifically when using periapical radiography, a technique designed for evaluating osseointegration in dental implants.

Therefore, this study aimed to analyze the density and microstructure of the osseointegration process in dental implants, both with and without the addition of gambir (Uncaria gambir Roxb.), through periapical radiography. The method used was an observational analytic comparative with a cross-sectional design involving a total sampling of rabbit tibia bone with dental implants installed on days 3, 14, and 28. In total, 24 periapical radiography images of the samples, taken over a span of 28 days, were selected using a total sampling technique, covering both gambir and control groups.

The normality test was performed using the Shapiro-Wilk test, the qualitative assessment employed the Mann-Whitney test, and the quantitative assessment involved one-way ANOVA along with post hoc tests. The results showed that the average values per time in both gambir and control groups had p-values > 0.05 for all variables. However, for bone volume/total volume (BV/TV) in the control group over time, the p-value was < 0.05. A descriptive trend emerged, showing superior values in density and microstructure between gambir and control groups across different time intervals of days 3, 14, and 28 when employing periapical radiography. Additionally, it was important to note that no statistically significant differences were observed.

**Clinical article (J Int Dent Med Res 2024; 17(1): 232-238)**

**Keywords:** Osseointegration, Dental implant, Periapical Radiograph, Uncaria Gambir Roxb.

**Received date:** 29 October 2023 **Accept date:** 06 January 2024

## Introduction

The popularity of dental implant treatment among the public is increasing and projected to continue rising until 2026. In Indonesia, the prevalence of the usage of this device is expected to reach 0.2% by the same year.[1] Implant failure often originates from infections, with peri-implantitis being the most common, affecting 34% of patients. Furthermore, the dental implant failure rate associated with this infection was 3.11%.[2] Due to the high cost of dental implant treatment, precise and accurate evaluations are imperative. The efficiency of the device can be evaluated through various parameters, such as minimal bone loss in radiographic images.[3]

Gambir plant (Uncaria gambir Roxb.), which often grows in abundance in Indonesia, has drawn attention.[4] Its extract contains several flavonoid components, with catechin comprising a significant portion (7-33%).[4]Activity tests have shown that gambir catechin isolates exhibit various pharmacological activities, including antioxidant, antibacterial, and anti-inflammatory.[5-8]. The mechanism of flavonoids as anti-inflammatory agents involves inhibiting COX-2 enzymes to control pain and edema.[9,10] They also play a role in stimulating the formation of osteoblasts and osteoclasts during the remodeling phase, thereby aiding the implant osseointegration process.[11]

Osseointegration is a critical aspect and one of the prerequisites for the success of dental implants.[11,12] Furthermore, it closely correlates with the bone healing process, which consists of 3 phases, namely hemostasis and inflammation,

*Corresponding author:
Dr. Farina Pramanik, DDS., MSc
Department of Dentomaxillofacial Radiology, Faculty of Dentistry, Universitas Padjadjaran, Bandung, Indonesia.
E-mail: farina.pramanik@unpad.ac.id.

proliferation, as well as remodeling.[13,14] During the inflammation phase, the peak expression of TNF-α occurs on day 3 after implantation, followed by a subsequent decrease.[25] The highest BMP-2 gene expression after tooth extraction is observed between days 7 and 14, corresponding to the proliferation phase.[16] The remodeling process typically begins around day 21 and continues for 1 year or after 4 weeks. The outcomes observed were stabilization of bone remodeling around the implant and an increase in the amount of bone matrix.[14,17]

Assessment of density through the mean value of grey, fractal dimension (FD), and microstructure can provide insights into the osseointegration process in the bone. Microstructure parameters can directly, including bone volume over total volume fraction (BV/TV), trabecular thickness (Tb.Th), trabecular separation (Tb.Sp), and trabecular number (Tb.N), offer direct and accurate depictions of the bone osseointegration process.[18]

Periapical radiography offers several advantages, including cost-effectiveness, accuracy, widespread availability of tools in dental clinics and hospitals, minimal distortion, accurate image production, minimal superimposition, as well as detailed depiction.[19,20] Rabbits serve as a good model for bone investigations due to their close resemblance to human bone conditions.[21] Rabbit tibia bone used in this study was relatively small, allowing periapical radiography to provide a more focused image.[19,20]

The selection of day 3 as a time point was based on the peak expression of TNF-α after implantation, followed by a decrease.[22,23] Day 14 corresponds to the period of highest BMP-2 gene expression during the proliferation phase. Furthermore, the BMP-2 speed plays a role in osteogenesis.[16,24] Jaqueline et al. stated that microstructure values continued to improve over time until day 28. This aligned with the activities of osteoblast and osteoclast.[25]

Praneeth et al. conducted a study exploring various strategies to enhance osseointegration, such as using *Moringa oleifera* plant gel during dental implant placement. This led to new bone formation without degenerative changes and a shortened osseointegration period.15 Alghamdi investigated methods to improve osseointegration in low-quality bone (Type-IV) by applying drug coatings to the implant surface. The results indicated the need for surface modifications to enhance osseointegration within the bone.[26] Smeets et al. stated that surface modifications of dental implants were essential for minimizing bacterial adhesion, boosting osseointegration, and preventing peri-implantitis.[27]

According to previous investigations and insights, it becomes viable to consider a novel method by modifying the surface of dental implants using another natural element, such as gambir. Therefore, this study aimed to analyze the differences in osseointegration microstructure and density around dental implants in rabbit tibia. Periapical radiography images at different time intervals (days 3, 14, and 28), both with and without the addition of gambir.

## Materials and methods

This study was approved by the Animal Ethics Commission, Faculty of Veterinary Medicine, Bogor Agricultural University under the number 006/KEH/SKE/III/2021 as well as the Dental and Oral Hospital of Padjadjaran University under the number 224/UN6.RSGM/TU.00/2023. This study was conducted from January to March 2023, at the Oral and Dental Radiology Installation of the Dental and Oral Hospital, Padjadjaran University.

This study employed an observational analytic comparative method, using rabbit tibia bone with dental implants over 28 days. The population consisted of periapical radiography images of the samples, while the treatment was the addition of gambir extract. The inclusion criteria considered were clear periapical radiography images of rabbit tibia bone sections with dental implants at time intervals of 3, 14, and 28 days, both with and without the addition of gambir. Gambir extract was obtained from dry leave of Gambir and extracted in Chemistry Laboratory, Faculty of Chemistry, Padjadjaran University.[28] A total sampling method was employed in this study, resulting in a sample size of 24 periapical radiography images of rabbit tibia bone sections with dental implants, encompassing both those with and without gambir.

The following materials and tools were used: rabbit tibia bone sections with dental implants over a 28-day period, both with and without gambir; periapical digital focus

instrumentation format of the Cliniview software (Cliniview Software, Finland); conventional x-ray equipment, computer (Toshiba Portege Intel Core 13, Tokyo, Japan) with Windows 7 (Microsoft, Washington, USA); phosphor plate sensor; and red U-shaped clay used as the sample base.[27] Additionally, some other tools included a dental implant by dentist brand (DENTIS Co., LTD., Dong-gu, South Korea) made of Ti-alloy grade 4 with a length of 7 mm and diameter of 4 mm, over 3, 14, and 28 days, ImageJ (National Institutes of Health, US) software for analyzing density and microstructure, as well as SPSS 28.0.1 (SPSS, Chicago, Illinois, USA) software for data processing. The experimental setup involved in periapical radiography shows in Figure 1.

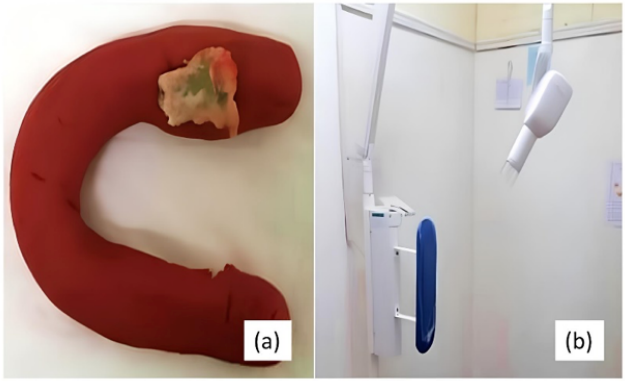


**Figure 1.** The experimental setup involved (a) Placing rabbit tibia bone in the molar region of a jaw model made of clay, and (b) Using a periapical radiography apparatus.

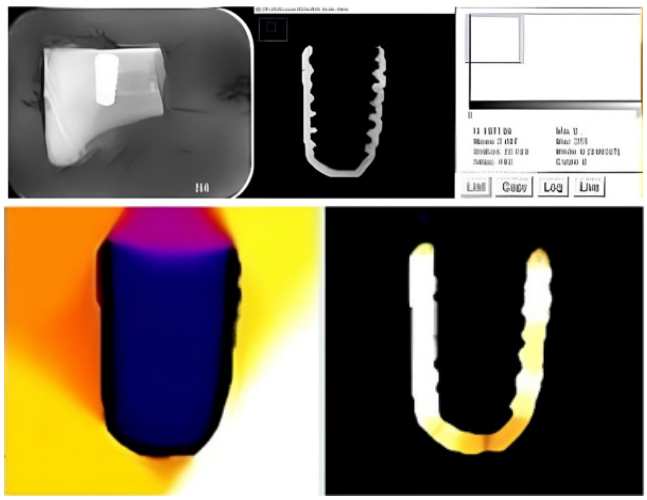

**Figure 2.** The use of ImageJ software to assess density and microstructure in bone osseointegration processes.

Data for this study was collected through observations. A total of 24 periapical radiography images of dental implants in rabbit tibia were quantitatively analyzed using ImageJ software. The use of ImageJ software to assess density and microstructure in bone osseointegration processes can be seen in Figure 2. The indicators assessed were density, FD, BV/TV, Tb.Th, Tb.Sp, and Tb.N, around the dental implants in rabbit tibia. The procedures involved opening the software, selecting periapical radiography images to be investigated, and creating a U-shaped region of interest (ROI) with a width of 1 mm using the freehand tool. Subsequently, the density, FD, Tb.Th, and Tb.Sp, as well as BV/TV, were analyzed using the histogram, fraclac, the local thickness, and the area/volume fraction plugin, respectively. Finally, Tb.N was calculated using formula 1/(Tb.Th + Tb.Sp), followed by the recording of both the data and analysis.

The differences in density and microstructure assessment in radiography images of dental implants with and without gambir were tested using the Mann-Whitney Test. This test was conducted to determine the presence or absence of a significant difference in the Mean of 2 independent samples. Due to the relatively low sample size in this study, a normality test was performed on the osseointegration assessment data, namely density, FD, BV/TV, Tb.Th, Tb.Sp, and Tb.N, using the Shapiro-Wilk test. Meanwhile, the paired t-test was conducted in 3 replications to examine the consistency of the assessment.

## Results

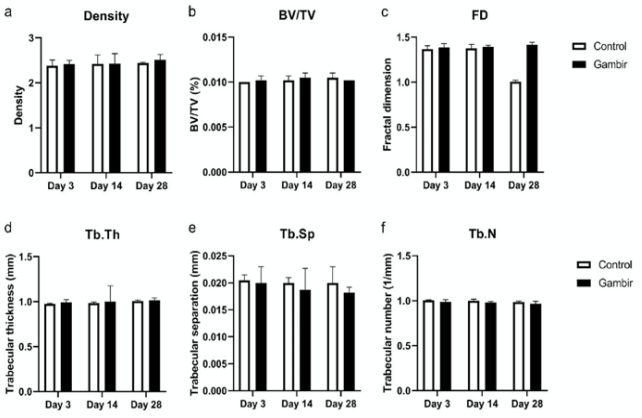


**Figure 3.** Effect of Gambir on bone density and microstructure (a) Density, (b) BV/TV, (c) Fractal dimension, (d) Trabecular thickness, (e) Trabecular separation, (f) trabecular number.
Data are shown as the mean ± standard deviation.

The sample was collected through the selection of subjects that met the inclusion criteria. Furthermore, it consists of 24 periapical radiography images of dental implants in rabbit tibia, both with and without gambir treatment, observed over time variations of 3, 14, and 28 days. The sample was assessed for density, BV/TV, FD, Tb.Th, Tb.Sp, and Tb.N. The osseointegration density and microstructure assessment results were shown in Figure 3.

Based on Figure 3, both of control and gambir treatment, the density(Figure 3a), BV/TV(Figure 3b), FD(Figure 3c), and Tb.Th(Figure 3d) values show an increase trend in treatment time manner, then the values of Tb.Sp(Figure 3e) and Tb.N(Figure 3f) were decrease in the treatment time manner trend. The BV/TV value, with gambir treatment, was increased from day 3 to 14 and decreased on day 28 (Figure 3(b)). In contrast, BV/TV value of control treatment was increased over time treatment. The normality test results for all variables are presented in Table 1. Table 2. Shows the comparison of each variable between treatments.

| Variable | Day 3 (p-value) | | Day 14 (p-value) | | Day 28 (p-value) | |
|---|---|---|---|---|---|---|
| | Gambir | Control | Gambir | Control | Gambir | Control |
| Density | 0.312 | 0.205 | 0.333 | 0.258 | 0.164 | 0.306 |
| BV/TV | 0.441 | 0.000 | 0.307 | 0.361 | 0.441 | 0.307 |
| FD | 0.380 | 0.188 | 0.228 | 0.441 | 0.207 | 0.352 |
| TbTh | 0.301 | 0.225 | 0.265 | 0.205 | 0.339 | 0.250 |
| TbSp | 0.236 | 0.283 | 0.275 | 0.293 | 0.441 | 0.236 |
| TbN | 0.298 | 0.298 | 0.333 | 0.260 | 0.358 | 0.296 |

**Table 1.** Normality test results for all variables.
Note: The p-value for the Shapiro-Wilk test was used to assess the normality of the data. When this value was less than 0.05, it indicated that the data were not normally distributed.

The results of the Shapiro-Wilk normality test on the 6 variables showed a normal distribution pattern for the data. Specifically, p-values greater than 0.05 were obtained for all variables, except for the control group data in the BV/TV variable on day 3, where it was less than 0.05. This signified that the data for this variable did not follow a normal distribution.

From Table 3, the analysis of variance (ANOVA) results between the different time points within each group showed p-values > 0.05. This signified the absence of significant differences among the time intervals and treatments. The Kruskal-Wallis test results for all variable values exhibited insignificant differences at each time interval, with p-values > 0.05.

| Variable | | Mean (SD) | | p-value* |
|---|---|---|---|---|
| | | Control | Gambir | |
| Density | Day 3 | 2.379 (±0.127) | 2.417 (±0.085) | 0.718 |
| | Day 14 | 2.418 (±0.203) | 2.423 (±0.227) | 0.964 |
| | Day 28 | 2.437 (±0.020) | 2.511 (±0.123) | 0.743 |
| BV/TV | Day 3 | 0.0100 (±0.0000) | 0.0102 (±0.0005) | 0.4762 |
| | Day 14 | 0.0102 (±0.0005) | 0.0105 (±0.0005) | 0.4762 |
| | Day 28 | 0.0105 (±0.0005) | 0.0102 (±0.0000) | 0.4762 |
| Fractal Dimension (FD) | Day 3 | 1.367 (±0.039) | 1.386 (±0.043) | 0.421 |
| | Day 14 | 1.377 (±0.043) | 1.394 (±0.015) | 0.457 |
| | Day 28 | 1.384 (±0.014) | 1.416 (±0.027) | 0.191 |
| Trabecular Thickness (TbTh) | Day 3 | 0.977 (±0.006) | 0.9937 (±0.029) | 0.255 |
| | Day 14 | 0.983 (±0.015) | 1.002 (±0.173) | 0.189 |
| | Day 28 | 1.006 (±0.012) | 1.014 (±0.028) | 0.558 |
| Trabecular Separation (TbSp) | Day 3 | 0.0205 (±0.001) | 0.0200 (±0.003) | 0.793 |
| | Day 14 | 0.0200 (±0.001) | 0.0187 (±0.004) | 0.529 |
| | Day 28 | 0.0200 (±0.003) | 0.0182 (±0.001) | 0.373 |
| Trabecular Number (TbN) | Day 3 | 1.004 (±0.008) | 0.987 (±0.026) | 0.221 |
| | Day 14 | 1.000 (±0.017) | 0.979 (±0.011) | 0.129 |
| | Day 28 | 0.985 (±0.012) | 0.968 (±0.027) | 0.709 |

**Table 2.** Comparison of each variable between treatments.

| Treatment | Comparison over time | p-value* | | | | | |
|---|---|---|---|---|---|---|---|
| | | Density | BV/TV | FD | TbTh | TbSp | TbN |
| Control | Day 3 & 14 | 0.998 | 0.976 | 0.998 | 0.997 | 1.000 | 1.000 |
| | Day 14 & 28 | 1.000 | 0.976 | 1.000 | 0.615 | 1.000 | 0.369 |
| | Day 3 & 28 | 0.977 | 0.695 | 0.977 | 0.382 | 1.000 | 0.242 |
| Gambir | Day 3 & 14 | 1.000 | 0.976 | 0.999 | 0.989 | 0.985 | 0.989 |
| | Day 14 & 28 | 0.957 | 0.976 | 0.939 | 0.955 | 1.000 | 0.961 |
| | Day 3 & 28 | 0.945 | 1.000 | 0.808 | 0.694 | 0.938 | 0.717 |

**Table 3.** Comparison of each variable over time.
Description: *) The p-value is obtained from the Analysis of Variance test (density, BV/TV, TbTh, TbN in both groups) except for BV/TV in the control group using the Kruskal-Wallis test.

## Discussion

In the context of the healing process, the evolution of bone structure over time is a dynamic phenomenon. In the initial phases, trabecular patterns appear thinner and more sparse, gradually thickening in subsequent phases.[29] The assessment of bone strength and structure often relied on factors such as mass, geometry, and quality.[30] For this study, BV/TV, FD, Tb.Th, Tb.Sp, and Tb.N were employed as measures of bone growth around implants.[31] FD offered insights into the intricate structural pattern

of bone in relation to its density value.[32] BV/TV represented the bone volume within the tissue volume.[33] During the healing phase, the sample was subjected to compaction and maturation to support its increasing volume.[17] Tb.Sp reflected the mean distance between trabecular bone, where narrower gaps correspond to higher density.[33] Meanwhile, Tb.Th represented the mean thickness of trabecular bone and is closely associated with increased values of BV/TV and Tb.N. Furthermore, it described the number of trabeculae per unit bone length.[33,34] This correlates with increased new bone formation, resulting in an augmentation of trabecular bone. The quality of bone evolves in accordance with conditions and time, influenced by factors such as hormones, vitamin intake, and mechanical properties.[29]

Gambir, containing flavonoids, acts as an anti-inflammatory agent by reducing the activity of the enzyme lipoxygenase, thereby inhibiting leukotriene activity and the activation of leukocytes during inflammation processes.[35] The plant can also inhibit cyclooxygenase enzymes, impeding prostaglandin formation and hindering the oxidation of arachidonic acid, which leads to the prevention of reactive oxygen and chemical mediators.[35] As a result, the inflammation process is accelerated and bone healing is facilitated. In this phase, the density and microstructure of bone are higher in gambir group compared to the control.

Previous studies indicated that osseointegration significantly impacted implant stability within the bone.[31] FD values showed an increase from the inflammation phase to day 28.[36] According to Jaqueline et al., BV/TV, Tb.Th, and Tb.N increased while Tb.Sp decreased over time until day 28, aligning with osteoblast and osteoclast activities.[24]

The osseointegration assessment results on days 3, 14, and 28 do not exhibit significant differences across all variables, thereby not demonstrating the quantitative effectiveness of gambir extract in the bone healing process at this point. The lack of significance was attributed to all variables having p-values > 0.05 in the paired t-test, variance, and Kruskal-Wallis tests. However, gambir and control groups, along with their developmental changes over time, showed better values at each phase. This aligned with literature indicating that the flavonoids in the plant were considered effective anti-inflammatory agents and expected to facilitate rapid osseointegration.[37]

Based on descriptive statistical calculations, the values for density and microstructure on days 3, 14, and 28 improved over time. Theoretically, on day 3, monocytes or macrophages penetrated the wound through the mediation of monocyte chemoattractant protein 1 (MCP-1). Macrophages secrete proteases to degrade the extracellular matrix (ECM), crucial for removing foreign materials, stimulating cell movement, and regulating ECM turnover.[14] Day 3 marks the inflammation phase in the bone healing process, with the highest expression of TNF-α occurring on this day. This increased expression leads to inflammation and inhibits osteoblast formation during bone development. On day 3, the periphery of the implant adjacent to the bone experiences hypoxia, causing an inflammation process. During this process, ion, water, and protein absorption occur. There was also an increase in Runx2, Wnt, TGF-β, Osterix, Osteocalcin, ALP, and Osteoprotegerin, which play roles in the maturation and inhibition of bone formation. Additionally, it inhibits COX-2, TNF-α, RANKL, TRAP Enzyme, Nf-Kb, Caspase-3 reaction, and Fenton reaction, regulating osteoclasts and degradation during inflammation. At this phase, the immature bone mesh was observed to develop from the endosteal origin to fill over half the bone marrow volume around the implant after 1 week.[24,28-42]

On day 14, Vascular Endothelial Growth Factor (VEGF), a potent angiogenic factor, was generated by keratinocytes, macrophages, and fibroblasts during the healing process.[13] During this phase, epithelialization occurred, involving the reconstruction of damaged layers.[19] The tissue scar remodeling phase was the longest in the healing process. According to Takeshita et al., the initial formation was resorbed after 14 days and replaced by mature flat bone, mostly in contact with the implant. Day 14 signified the proliferation phase with BMP-2 being the highest gene expression.[24,39,42]

On day 28, a significant transformation took place as the bone marrow space and trabeculae appeared thicker. This phenomenon arose as the bone matrix was densified, marked by the growth of mature bone fibers, known as lamellar bone, in the interface region between the dental implant and the surrounding bone. The maturation process was accompanied by the

formation of osteons.[42] During this phase, there was a noticeable decline in the levels of certain inflammatory cytokines, while others such as TNF, IL-1, and BMP-2 remained elevated.[43] This transition towards lower inflammation levels was reflected in radiographic images, which started to exhibit increased radiopacity. The density and microstructure values on day 28 tended to be higher, primarily due to the formation of a mature bone matrix and the maturation of collagen fibers. These changes marked the initiation of the osseointegration process, a critical step in implant stability. However, it is worth noting that Tb.Sp showed a further decrease at this phase, indicating a denser bone structure.[44] The remodeling process drastically enhanced wound resistance strength, and it was underpinned by the transformation from collagen type III to type I. A significant increase in strength occurred from weeks 3 to 6 after wound, with maximum wound resistance strength reaching 90% of normal tissue strength.[13]

Based on descriptive statistical calculations, the results showed that the values in gambir group were superior. This was consistent with the mechanism of flavonoids as anti-inflammatory agents, inhibiting COX-2 enzymes to control edema and pain. Furthermore, flavonoids were implicated in facilitating osteoblast and osteoclast formation during the remodeling phase for implant osseointegration.[8,9]

The quality characteristics of bone were assessed by analyzing its microstructure. According to Jaqueline et al., BV/TV, Tb.Th, and Tb.N consistently increased, while Tb.Sp decreased over time up to day 28, in line with osteoblast and osteoclast activity.[24] The quality of bone evolved in accordance with conditions and time, influenced by various factors such as hormones, vitamin intake, and mechanical properties.[27] The lack of a significant gambir effect could stem from intervention, such as infection, affecting the value and dose provided, which was not optimal for achieving the desired results. An optimal dose of flavonoids was expected to yield positive results for bone health.[45]

Analysis based on 2D image measurements using ImageJ software heavily depended on the regions of interest (ROIs) selected, making it a challenging procedure.[29] Delphine P Antony et al. stated that periapical radiography, CBCT, and panoramic radiography had an accuracy of 70, 91.3, and 54%, for detecting bone structure.[46] However, the periapical radiography apparatus remained significant and served as a foundation for decision-making in the assessment of dental implant osseointegration. This would be followed by further examinations using electron microscopy and histomorphometry analysis.

## Conclusions

In conclusion, osteointegration evaluation of dental implant osseointegration in rabbit tibia with and without gambir was performed using 24 periapical radiographic images. The results showed a descriptive trend with better values in density and microstructure (density BV/TV, FD, Tb.Th, TbSp, and Tb.N) between the two treatments (gambir and control groups) and various time intervals of days 3, 14, and 28. However no statistically significant differences were observed between grops.

## Acknowledgements

The authors would like to thank the Department of Dentomaxillofacial Radiology and Doctoral Program S3, Faculty of Medicine of Padjajaran University, for all the kind support of the study.

## Declaration of Interest

The authors report no conflict of interest.

## References

1.Berniyanti T, Palupi R, Alkadasi BA, et al. Oral Health-Related Quality of Life (OHRQoL) Analysis in Partially Edentulous Patients with and without Denture Therapy. Clin Cosmet Investig Dent. 2023;15:89-98.
2.Thiebot N, Hamdani A, Blanchet F, Dame M, Tawfik S, Mbapou E, et al. Implant failure rate and the prevalence of associated risk factors: A 6-year retrospective observational survey. J Oral Med Oral Surg. 2022;28(2):1–8.
3.Papaspyridakos P, Chen CJ, Singh M, Weber HP, Gallucci GO. Success criteria in implant dentistry: A systematic review. J Dent Res. 2012;91(3):242–8. 4.
4.Munggari IP, Kurnia D, Deawati Y, Julaeha E. Current Research of Phytochemical, Medicinal and Non-Medicinal Uses of Uncaria gambir Roxb.: A Review. Molecules. 2022;27(19):6551
5.Yunarto N, Intan PR, Kurniatri AA, Sulistyowati I, Aini N. Anti-Inflammatory Activities of Ethyl Acetate Fraction From Uncaria Gambir Leaves Through the Inhibition of Edema, COX-2 and iNOS Expression. 2020;22(Ishr 2019):108–12.
6.Khan MS, ur Rehman S, Ali MA, Sultan B, Sultan S. Infection in orthopedic implant surgery, its risk factors and outcome. J Ayub Med Coll Abbottabad. 2008;20(1):23–5.

7. Bartoli CR, Godleski JJ. Blood flow in the foreign-body capsules surrounding surgically implanted subcutaneous devices. J Surg Res. 2010;158(1):147–54.
8. Pachimalla PR, Mishra SK, Chowdhary R. Evaluation of hydrophilic gel made from Acemannan and Moringa oleifera in enhancing osseointegration of dental implants. A preliminary study in rabbits. J Oral Biol Craniofacial Res. 2020;10(2):13–9.
9. Polito F, Bitto A, Irrera N, Squadrito F, Fazzari C, Minutoli L, et al. Flavocoxid, a dual inhibitor of cyclooxygenase-2 and 5-lipoxygenase, reduces pancreatic damage in an experimental model of acute pancreatitis. Br J Pharmacol. 2010;161(5):1002–11.
10. Panche AN, Diwan AD, Chandra SR. Flavonoids: an overview. J Nutr Sci. 2016;5:e47.
11. Jayesh RS, Dhinakarsamy V. Osseointegration. J Pharm Bioallied Sci. 2015;7(Suppl 1):S226-S229.
12. Parithimarkalaignan S, Padmanabhan T V. Osseointegration: An update. J Indian Prosthodont Soc. 2013;13(1):2–6.
13. Tottoli EM, Dorati R, Genta I, Chiesa E, Pisani S, Conti B. Skin Wound Healing Process and New Emerging Technologies for Skin Wound Care and Regeneration. Pharmaceutics. 2020;12(8):735-765.
14. Ritsu M, Kawakami K, Kanno E, Tanno H, Ishii K, Imai Y, et al. Critical role of tumor necrosis factor- α in the early process of wound healing in skin. J Dermatology Dermatologic Surg. 2017;21(1):14–9.
15. Sukmana BI, Budhy TI, Ardani IGAW. The potentiation of Mangifera casturi bark extract on interleukin- 1β and bone morphogenic protein-2 expressions during bone remodeling after tooth extraction. Dent J (Majalah Kedokt Gigi) [Internet]. 2017;50(1):36–42.
16. Wang L, Gao Z, Su Y, Liu Q, Ge Y, Shan Z. Osseointegration of a novel dental implant in canine. Sci Rep. 2021 Feb;11(1):4317.
17. Krug R, Carballido-Gamio J, Burghardt AJ, Kazakia G, Hyun BH, Jobke B, et al. Assessment of trabecular bone structure comparing magnetic resonance imaging at 3 Tesla with high-resolution peripheral quantitative computed tomography ex vivo and in vivo. Osteoporos Int. 2008;19(5):653–61.
18. Masthoff M, Gerwing M, Masthoff M, et al. Dental Imaging - A basic guide for the radiologist. Dentale Bildgebung – Eine Einführung für den Radiologen. Rofo. 2019;191(3):192-198.
19. Widyaningrum R, Lestari S, Jie F. Image analysis of periapical radiograph for bone mineral density prediction. Int J Electr Comput Eng. 2018;8(4):2083–90.
20. Schafrum Macedo A, Cezaretti Feitosa C, Yoiti Kitamura Kawamoto F, Vinicius Tertuliano Marinho P, dos Santos Dal-Bó Í, Fiuza Monteiro B, et al. Animal modeling in bone research—Should we follow the White Rabbit? Anim Model Exp Med. 2019;2(3):162–8.
21. Cheng AW, Tan X, Sun JY, Gu CM, Liu C, Guo X. Catechin attenuates TNF-α induced inflammatory response via AMPK-SIRT1 pathway in 3T3-L1 adipocytes. PLoS One. 2019;14(5):1–15.
22. Osta B, Benedetti G, Miossec P. Classical and paradoxical effects of TNF-α on bone homeostasis. Front Immunol. 2014;5:1–9.
23. Xu B, Wang X, Wu C, Zhu L, Chen O, Wang X. Flavonoid compound icariin enhances BMP-2 induced differentiation and signalling by targeting to connective tissue growth factor (CTGF) in SAMP6 osteoblasts. PLoS One. 2018;13(7):1–16.
24. Hassumi JS, Mulinari-Santos G, Fabris AL da S, Jacob RGM, Gonçalves A, Rossi AC, et al. Alveolar bone healing in rats: micro-CT, immunohistochemical and molecular analysis. J Appl Oral Sci. 2018;26:e20170326.
25. Alghamdi HS. Methods to improve osseointegration of dental implants in low quality (type-IV) bone: An overview. J Funct Biomater. 2018;9(1):7.
26. Smeets R, Stadlinger B, Schwarz F, et al. Impact of Dental Implant Surface Modifications on Osseointegration. Biomed Res Int. 2016;2016:6285620.
27. Chang PC, Lang NP, Giannobile WV. Evaluation of functional dynamics during osseointegration and regeneration associated with oral implants. Clin Oral Implants Res. 2010;21(1):1-12.
28. Lubis RT, Azhari A, Pramanik F. Analysis of Bone Density and Bone Morphometry by Periapical Radiographs in Dental Implant Osseointegration Process. Int J Dent. 2023;2023:4763961.
29. da Silva AMH, Alves JM, da Silva OL, da Silva Junior NF. Two and three-dimensional morphometric analysis of trabecular bone using X-ray microtomography (μCT). Rev Bras Eng Biomed. 2014;30(2):93–101.
30. He T, Cao C, Xu Z, Li G, Cao H, Liu X, et al. A comparison of micro-CT and histomorphometry for evaluation of osseointegration of PEO-coated titanium implants in a rat model. Sci Rep. 2017;7(1):1–11.
31. Soylu E, Coşgunarslan A, Çelebi S, Soydan D, Demirbaş AE, Demir O. Fractal analysis as a useful predictor for determining osseointegration of dental implant? A retrospective study. Int J Implant Dent. 2021;7(1)14.
32. Lee JH, Chun KJ, Kim HS, Kim SH, Han P, Jun Y, et al. Alteration patterns of trabecular bone microarchitectural characteristics induced by osteoarthritis over time. Clin Interv Aging. 2012;7:303–12.
33. Keaveny TM, Yeh OC. Architecture and trabecular bone - Toward an improved understanding of the biomechanical effects of age, sex and osteoporosis. J Musculoskelet Neuronal Interact. 2002;2(3):205–8.
34. Septiani D, Yuslianti R, Lenggogeni S, Departemen N, Biologi O, Kedokteran F, et al. Effect of Ethanol Gambir Leaves (Uncaria Gambir) Compared With Chlorhexidine Gluconate 0,2% Topical for Wound Healing on Palate Mucosal Galur Wistar Rat. dentika Dent J. 2015;18(3):262–7.
35. Xu H, Zhang J, Jiang Y, Lu S, Niu Y, Dong J, et al. Fractal analysis of rat dermal tissue in the different injury states. Int Wound J. 2022;19(5):1016-1022.
36. Borquaye LS, Laryea MK, Gasu EN, Boateng MA, Baffour PK, Kyeremateng A, et al. Anti- inflammatory and antioxidant activities of extracts of Reissantia indica, Cissus cornifolia and Grosseria vignei . Cogent Biol. 2020;6(1):1785755.
37. Oikonomidou PR, Casu C, Yang Z, Crielaard B, Shim JH, Rivella S, et al. Polycythemia is associated with bone loss and reduced osteoblast activity in mice. Osteoporos Int. 2016;27(4):1559–68.
38. Huang HT, Cheng TL, Lin SY, Ho CJ, Chyu JY, Yang R Sen, et al. Osteoprotective roles of green tea catechins. Antioxidants. 2020;9(11):1–25.
39. Komori T. What is the function of osteocalcin? J Oral Biosci. 2020;62(3):223–7.
40. Sinha KM, Zhou X. Genetic and molecular control of osterix in skeletal formation. J Cell Biochem. 2013;114(5):975–84.
41. Boyce BF, Xing L. Functions of RANKL/RANK/OPG in bone modeling and remodeling. Arch Biochem Biophys. 2008;473(2):139–46.
42. Bahney CS, Zondervan RL, Allison P, Theologis A, Ashley JW, Ahn J, et al. Cellular biology of fracture healing. J Orthop Res. 2019;37(1):35–50.
43. Claes L, Recknagel S, Ignatius A. Fracture healing under healthy and inflammatory conditions. Nat Rev Rheumatol. 2012;8(3):133–43.
44. Biguetti CC, Cavalla F, Silveira EM, Fonseca AC, Vieira AE, Tabanez AP, et al. Oral implant osseointegration model in C57BL/6 mice: microtomographic, histological, histomorphometric and molecular characterization. J Appl Oral Sci. 2018;26:1–16.
45. Weaver CM, Alekel DL, Ward WE, Ronis MJ. Flavonoid Intake and Bone Health. J Nutr Gerontol Geriatr. 2012;31(3):239–53.
46. Antony DP, Thomas T, Nivedhitha M. Two-dimensional Periapical, Panoramic Radiography Versus Three-dimensional Cone-beam Computed Tomography in the Detection of Periapical Lesion After Endodontic Treatment: A Systematic Review. Cureus. 2020;12(4).